# Strong-field-ionization suppression by light-field control

Esa Räsänen[1,2] and Lars Bojer Madsen[3]

[1]*Department of Physics, Tampere University of Technology, FI-33101 Tampere, Finland*

[2]*Nanoscience Center, Department of Physics, University of Jyväskylä, FI-40014 Jyväskylä, Finland*

[3]*Lundbeck Foundation Theoretical Center for Quantum System Research, Department of Physics and Astronomy, Aarhus University, DK-8000 Aarhus C, Denmark*

(Received 6 July 2012; published 25 September 2012)

In recent attempts to control strong-field phenomena such as molecular dissociation, undesired ionization sometimes seriously limited the outcome. In this work we examine the capability of quantum optimal control theory to suppress the ionization by rational pulse shaping. Using a simple model system and the ground-state occupation as the target functional, we show that optimal control generally leads to a significant suppression of the ionization, although the fluence and the pulse length are kept fixed. In the low-frequency regime the ionization is reduced mainly by avoiding high peaks in the intensity and thus preventing tunneling. In contrast, at high frequencies in the extreme ultraviolet regime the optimized pulses strongly couple with the (de)-excitations of the system, which leads to different pulse characteristics. Finally, we show that the applied target functional works, to some extent, for the enhancement of the high-order-harmonic generation, although further developments in optimal control theory to find proper target functionals are required.

DOI: 10.1103/PhysRevA.86.033426 PACS number(s): 32.80.Qk, 32.80.Rm, 33.80.Rv, 42.50.Hz

## I. INTRODUCTION

During the last decade intense infrared (IR) femtosecond pulses and weak extreme ultraviolet (XUV) attosecond pulses have been used to manipulate, control, and monitor electron dynamics in real time [1]. For example, the so-called attosecond streaking technique was used to measure a time delay of around 20 as between ionization from the $2s$ and $2p$ orbitals in neon atoms [2], and an interferometric technique based on trains of attosecond pulses (resolution of attosecond beating by interference of two-photon transitions, RABBIT) was used to measure a delay of around 100 as for ionization between $2s$ and $2p$ orbitals in argon [3]. We refer the reader to Ref. [1] for a discussion of more applications, including, e.g., the experimental investigation of time-resolved tunneling ionization [4].

A few-cycle intense femtosecond pulse can by itself also be used for control. As a representative example we mention control of electron localization in molecular dissociation [5]. In such studies the control over the carrier-envelope phase (CEP) and the highly nonlinear response of the system to the external field are the key ingredients. For example, if the CEP, in the reproducible wave form, is varied such that the field reaches a much higher value during a single half cycle than during the rest of the pulse, ionization will be mainly confined to a fraction of that half cycle and hence controlled. If the wave form is not controlled, the latter temporal confinement of the main ionization events can be used experimentally to determine the CEP [6].

Generally, with optical and IR fields the manipulation and control of electron dynamics on the natural time scale require that the light fields are shaped on the subcycle level. Very recently, experimental progress on such subcycle shaping was reported [7]. It was demonstrated that subcycle transients of an intense femtosecond light field can be produced across the infrared, visible, and ultraviolet frequency regimes in a synthesized fashion. Such ultrafast manipulation of the light field opens up new possibilities for control of electron motion. In the present work we investigate such a question: is it possible, keeping the pulse duration and the fluence (energy) of an intense femtosecond pulse fixed, to significantly reduce the ionization by pulse shaping. We address this question by applying optimal control theory [8,9] (OCT) with different pulse constraints to a model system representing a one-dimensional hydrogen atom. The answer is affirmative, but the optimal procedure strongly depends on the frequency constraints. In the low-frequency regime the significant suppression of the ionization arises from the reduction of the peak intensity, which consequently reduces ionization by tunneling. In the high-frequency (UV) regime, on the other hand, complex (de)-excitation processes can be observed that efficiently prevent ionization. Finally, we analyze and discuss the connection of the present target functional with the control of the high-order-harmonic generation.

This paper is organized as follows. In Sec. II, we introduce OCT, our numerical techniques, and the model system. In Sec. III we present our results, which are split into four parts comprising a set of reference data without optimization (Sec. III A), OCT results in the low-frequency regime (Sec. III B) and in the high-frequency regime (Sec. III C), and the relevance of our results in terms of high-order-harmonic generation (Sec. III D). The paper is summarized in Sec. IV.

## II. THEORY AND MODEL

### A. Optimal control theory

OCT is a powerful method for finding optimized external fields such as laser pulses that drive the system to a predefined target with the maximum yield [8,9]. This can be done through iterating the time-dependent Schrödinger equation (TDSE) without any approximations apart from those imposed on the system itself, e.g., in terms of a model potential. Several OCT algorithms exist and their applicability depend on the type of the target functional and the applied field constraints. Here, to suppress ionization, our target is to maximize the ground-state

 

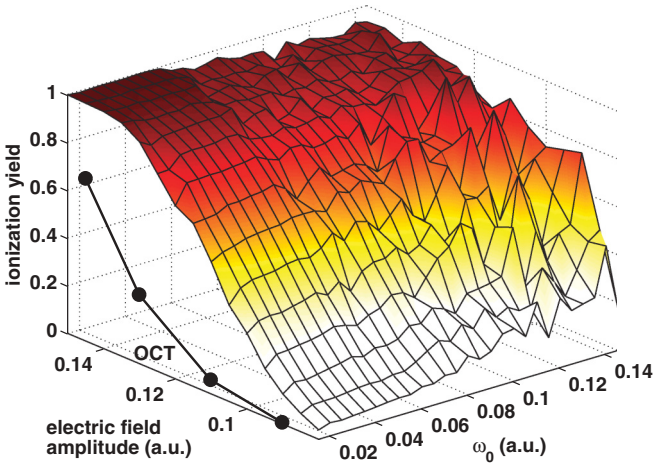


FIG. 1. (Color online) Ionization yield as a function of the pulse electric-field amplitude and frequency in a one-dimensional model atom. The pulse length is fixed to $T = 826.8$ (20 fs). The results from OCT are shown as solid circles. The OCT pulses have the same fluence and length as the nonoptimized ones, but they contain several frequencies up to $\omega_{\max} = 0.0654$ a.u. (700 nm).

(GS) occupation at the end of the pulse, so that the target operator has the form $\hat{O} = |\psi_0\rangle\langle\psi_0|$, where $|\psi_0\rangle$ is the GS. Hence, the target functional $J_1$ becomes a simple overlap between the GS and the time-dependent wave function $|\psi(t)\rangle$ at the end of the pulse $t = T$:

$$J_1 = \langle\psi(T)|\hat{O}|\psi(T)\rangle = |\langle\psi(T)|\psi_0\rangle|^2. \quad (1)$$

A more complete target to prevent ionization would consist of a larger set of bound states in the system, but the practical gain would be relatively small compared with the increased complexity of the optimization. However, throughout this paper we assess the ionization yield as 1 minus the projection to ten lowest eigenstates. In most cases, this is very close to the result obtained by subtracting only the ground-state occupation instead. For example, in the results shown in Fig. 1, the combined excited-state occupation remains within a few percentage points.

In this work we apply two different algorithms within OCT. First, we use a direct optimization scheme [10], where we construct a merit function

$$M(p) = \langle\psi_p(T)|\hat{O}|\psi_p(T)\rangle, \quad (2)$$

where $p$ is a set of parameters of the laser pulse. The merit function is maximized in the set $p$ with the derivative-free NEWUOA algorithm [11] by performing consecutive TDSE calculations. When using this algorithm, we express the laser pulse in the Fourier basis:

$$\epsilon(t) = \sum_{n=1}^{N}\left[\epsilon_n\sqrt{\frac{2}{T}}\cos(\omega_n t) + \gamma_n\sqrt{\frac{2}{T}}\sin(\omega_n t)\right], \quad (3)$$

where $\omega_n = 2\pi n/T$. The requirement for a conventional laser pulse, $\int_0^T dt\,\epsilon(t) = 0$, is now satisfied. Furthermore, the condition $\epsilon(0) = \epsilon(T)$ is guaranteed by setting $\sum_{n=1}^{N}\epsilon_n = 0$. The sum in Eq. (3) is truncated according to the maximum allowed frequency $\omega_{\max}$. The energy carried by the field (fluence, or time-integrated intensity) is limited to

$$F_0 = \int_0^T \epsilon^2(t)\,dt = \sum_{n=1}^{N}\left(\epsilon_n^2 + \gamma_n^2\right). \quad (4)$$

As our second algorithm we apply the scheme of Werschnik and Gross [12] (WG05), which is closer to the original OCT formulation exploiting efficient forward-backward propagation schemes [8,9]. Here the temporal pulse shape is freely varied without being restricted to a basis. The WG05 algorithm is often significantly more efficient than the above described direct control, especially when a relatively large frequency threshold $\omega_{\max}$ is applied. In WG05 this constraint is expressed in terms of a filter function [9].

We point out that for both OCT algorithms, i.e., for the direct and WG05 methods, we solve the full TDSE so that there are no approximations in that respect.

### B. Model system

We consider a one-dimensional model atom with the Hamiltonian

$$H(x,t) = -\frac{1}{2}\frac{\partial^2}{\partial x^2} - \frac{1}{\sqrt{1+x^2}} + x\epsilon(t), \quad (5)$$

where the second term is the static soft-Coulomb potential and the last term describes the electric field in the dipole approximation. The one-dimensional model [13] has been useful in the literature to analyze, e.g., multiphoton ionization [14]. Although the spectrum is very different from a full three-dimensional system (which is the subject of a future presentation), we believe that the qualitative features in the optimization processes are similar.

The TDSE is solved in real space on a grid using Krylov subspace projection and the exponential midpoint rule for the approximation of the propagator at $t + \Delta T$ [15]. All calculations are done with the OCTOPUS code [16]. The grid spacing and the time step are varied in the range $dx = 0.1 \cdots 0.2$ and $dt = 0.01 \cdots 0.05$, respectively. The numerical box size is varied between 200 and 400 a.u., and the box is surrounded by absorbing boundaries of a $\sin^2$-type imaginary potential.

## III. RESULTS

### A. Reference data

Before demonstrating the capabilities of OCT to suppress ionization we produce an extensive set of reference data. We compute the ionization yields of our model atom exposed to simple single-frequency pulses with a cosinoidal envelope and a fixed length of $T = 826.8$ a.u. (20 fs). This is a typical pulse length in recently synthesized light transients from the NIR to the UV regime [7].

Figure 1 shows the ionization yield, approximated here as 1 minus the projection to the ten lowest eigenstates, as functions of the electric field amplitude and the frequency. At low frequencies we find a smooth increase in the ionization as a function of the field amplitude, whereas the dynamics is much more complex at higher $\omega_0$, giving rise to a more complicated functional behavior in Fig. 1. This is simply due

to the coupling of the higher frequencies to the excitation energies, either directly or through a multiphoton process. Related to this effect, it is illuminating to see that at small amplitudes the ionization is enhanced as a function of $\omega_0$, whereas the behavior is opposite at large amplitudes; here the tunneling ionization is most effective at low frequencies when the field does not variate strongly in time.

The dependencies in Fig. 1 can be qualitatively analyzed with the commonly used Keldysh parameter $\gamma = \sqrt{I_p/2U_p}$ [17], where $I_p$ is the ionization potential and $U_p = I_0/(4\omega_0^2)$ is the ponderomotive energy with $I_0$ as the peak intensity. The tunneling and multiphoton regimes are characterized by $\gamma \ll 1$ and $\gamma \gg 1$, respectively. In Fig. 1 we indeed find that in the "smooth" regime with $\omega_0 \lesssim 0.06$ a.u. we have $\gamma \lesssim 0.5$, indicating the tunneling effect. A large part of the region plotted in Fig. 1 has $\gamma \sim 1$, and the clearest multiphoton regime is in the lower-right corner, with $\gamma \sim 2$.

### B. Low-frequency regime

Our OCT results for *minimizing* the ionization, obtained with the direct optimization scheme, are marked in Fig. 1 as solid circles. The fluence is fixed to the same values as in the nonoptimized results; in other words, the optimized pulse is forced to carry the same energy as the nonoptimized one. However, freedom in the frequency range is allowed: the threshold frequency is set to $\omega_{\max} = 0.0654$ a.u. (700 nm). The ability of OCT to suppress ionization is remarkable. For example, with the fluence $F_0 = 2.5$ a.u. (initial electric-field amplitude 0.11 a.u.) the optimally suppressed ionization yield is 6%, whereas the best nonoptimized result, i.e., the minimum ionization yield through the whole frequency range, is 55%.

Figure 2(a) shows the optimized pulse of the above-mentioned example in comparison with the initial pulse ($\omega_0 = 0.0459$ a.u.), both having the same fluence $F_0 = 2.5$ a.u. As the main observation, the optimization significantly reduces the peak intensity, and to account for the required fixed fluence, it introduces low-frequency components, which are shown in detail in the Fourier spectrum in Fig. 2(b). The phenomenon is well understandable due to the fact that in the tunneling regime the ionization probability is known to reach its maximum at peak intensities. A numerical demonstration of this effect was given in a previous work that focused on *enhancing* the ionization through OCT; it was found that optimization led to sharp peak intensities [10].

Figure 2(c) shows the GS occupation during the interaction with the laser pulse. The initial and optimized processes lead to 37% and 94% final GS occupations, respectively. Taking into account the negligible occupation of excited states in this example, the respective ionization yields are 63% and 6%. The effect of the electric field amplitude peaks in the nonoptimized pulse [dashed line in Fig. 2(a)] is clear in the GS occupation: at each local maximum with electric field amplitude ∼0.1 a.u. the GS occupation reduces by 10–20 percentage points.

We point out that in the IR-visible regime, i.e., at relatively low frequencies, the optimization process is generally similar to the above example, regardless of the precise characteristics of the initial pulse and the frequency threshold of the optimized pulse: OCT "flattens" out the pulse to avoid intensity peaks, and consequently, the pulse spectrum shifts to lower

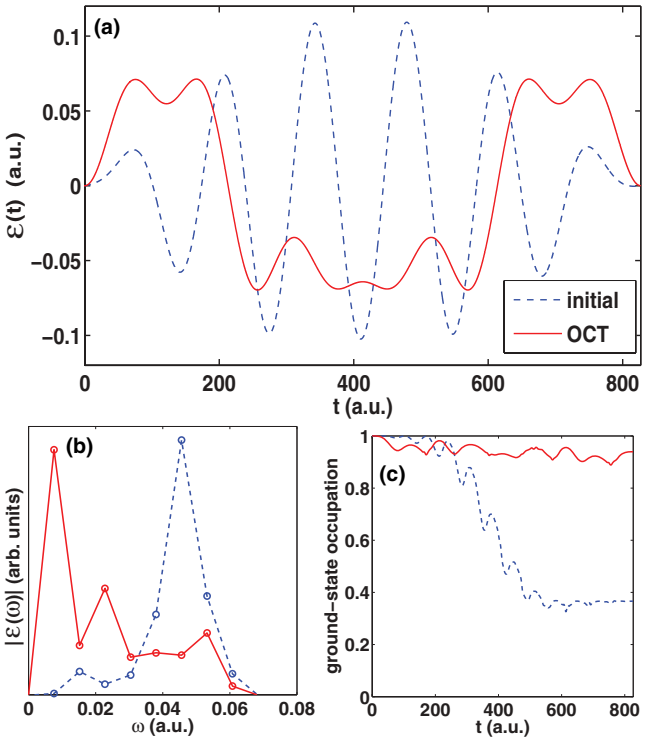


FIG. 2. (Color online) (a) Initial laser pulse with $\omega_0 = 0.0459$ a.u. (dashed line) and the optimized pulse (solid line) with a fixed fluence $F_0 = 2.5$. The resulting ionization yields are about 60% and 6%, respectively. (b) Fourier spectra of the pulses. (c) Occupation of the ground state during the process.

frequencies. We may conjecture that this tendency is general in the tunneling regime with $\gamma \ll 1$. In the following we consider the high-frequency regime where excitation processes are important in the optimization.

### C. High-frequency regime

Here we apply the WG05 algorithm (Sec. II A). The pulse length is fixed to 5 fs, and the initial frequency is fixed to $\omega_0 = 0.4$ a.u. This value is in the UV regime and close to the first excitation energy $\Delta E_{01} = 0.395$ a.u. The fluence is set to $F_0 = 1.16$ a.u., corresponding to the electric-field peak amplitude 0.15 a.u. in the initial pulse plotted in Fig. 3(a) (dashed line). As expected we find Rabi-like oscillations between the GS and the first excited state, although the occupation is gradually lost to higher states and to the continuum [see Fig. 3(b)]. The final GS occupation is 48%, and the first excited state has 12% population. As the higher states have negligible occupations, the ionization yield can be estimated to be ∼40%.

The optimized pulse in Fig. 3(a) (solid line) is, at first sight, similar to the initial one. In this case, however, the occupations evolve in a way such that the final GS occupation (and the total occupation) is as high as 91%. Hence, the ionization yield is only 9%, which is a remarkable improvement from the initial, nonoptimized result. A closer look at the occupations reveal that several states are involved in the optimized process; first, second, and third excited states reach respective (instant) maximum occupations of 80%, 34%, 12%, and 7.5% during the laser interaction. In contrast to the low-frequency regime

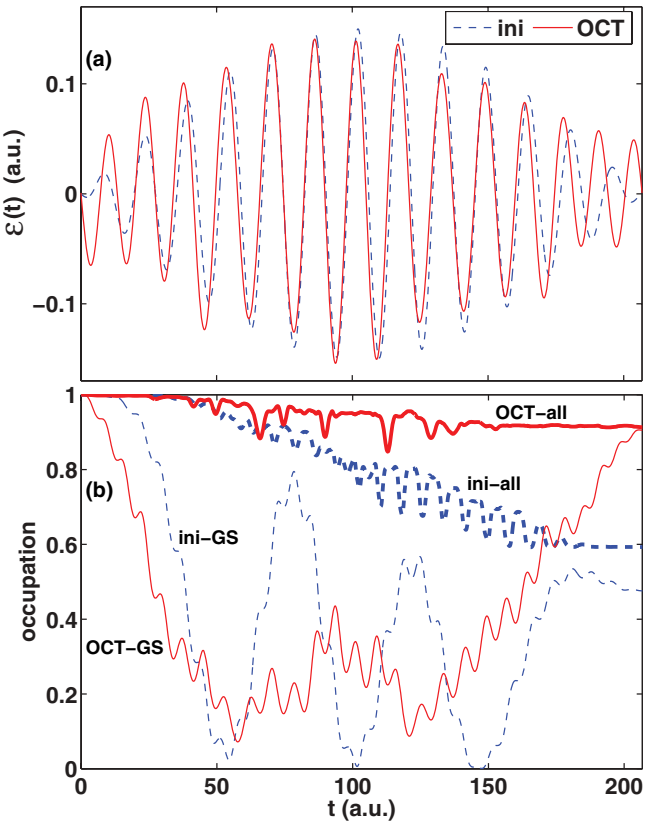


FIG. 3. (Color online) (a) Initial laser pulse with $\omega_0 = 0.4$ a.u. (dashed line) and the optimized pulse (solid line) with a fixed fluence $F_0 = 1.6$. (b) GS and total bound-state occupations during the initial (ini) and optimized (OCT) pulses. The resulting ionization yields are about 40% and 9%, respectively.

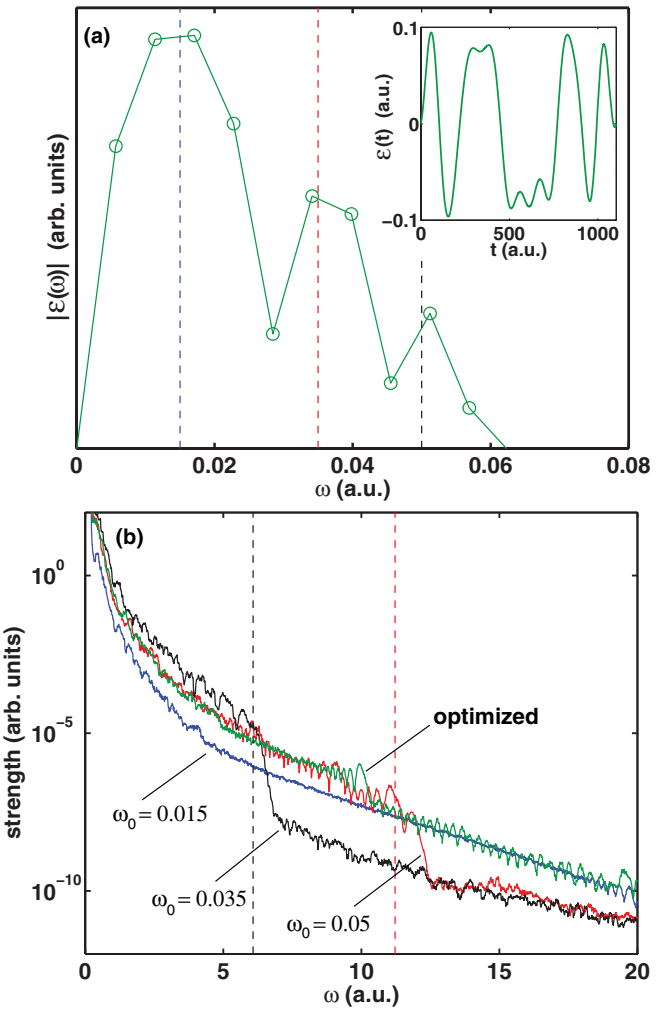


FIG. 4. (Color online) (a) Spectrum of the optimized pulse (inset) to maximize the ground-state occupation. (b) HHG spectrum obtained with the optimized pulse in (a) compared with the results from three single-frequency pulses having the dominant frequencies of the optimized pulse [dashed lines in (a)]. The theoretical HHG cutoffs for pulses with $\omega_0 = 0.035$ and 0.05 are marked by dashed lines in (b).

considered in the previous section, the peak intensities are now almost the same (in the OCT pulse even slightly higher). Now, the main optimization effect yielding the suppressed ionization arises from the shaping of the pulse envelope. OCT shapes the pulse in such a way that several bound-state (de)-excitation processes take place in the system during the pulse propagation in order to prevent driving the electron density to the continuum.

### D. Relation to the high-order-harmonic generation

Finally, we discuss a possible application of the ability to suppress ionization in strong fields within the process of high-order-harmonic generation (HHG). According to the three-step model [18], one might except that a high GS occupation at the end of the laser interaction could work as a target to enhance the HHG yield and/or the cutoff due to an efficient recombination (see also Ref. [19]).

We use the direct OCT algorithm (Sec. II A) with the pulse length $T = 1104.3$ a.u. (26.7 fs) and the initial frequency $\omega_0 = 0.0569$ a.u. (800 nm), which is set also as the maximum frequency in the optimization, i.e., $\omega_{\max} = \omega_0$. The resulting pulse and its spectrum are shown in Fig. 4(a). In this case the optimization increases the final GS occupation from 11% to 44%.

The HHG spectrum produced by the optimized pulse, calculated here as the squared Fourier transform of the dipole acceleration, is plotted in Fig 4(b). For clarity, we show the HHG spectrum as a 20-point moving average. To assess its quality we compare it with HHG spectra obtained from the main "components" of the optimized pulse, i.e., single-frequency pulses with $\omega_0 = 0.015$, 0.035, and 0.05, indicated by dashed lines in Fig. 4(a). The fluence is kept fixed in all four cases. For the single-frequency pulses the theoretical HHG cutoffs can be calculated from $E_{\text{cutoff}} = I_p + 3.17U_p$ (Ref. [20]), and they are marked by dashed lines in Fig. 4(b) (for $\omega_0 = 0.015$ the cutoff is at ∼58 a.u. and thus not visible). Interestingly, the optimized pulse yields a HHG spectrum that has overall a rather high yield through a large range of orders. However, it would be premature to claim that the present target functional (GS occupation) would be an optimal one to enhance the HHG yield or cutoff. Rather, the present target should be combined with a capability to (partly) ionize the system during the laser interaction and/or then to maximize

the *current* close to the core at the end of the pulse. This is the subject of future work within OCT in the strong-field regime.

## IV. SUMMARY

In summary, we have studied the possibilities of quantum optimal control theory to suppress the ionization of a model atom subjected to strong fields. The topic has relevance in view of applications to control, e.g., molecular dissociation or high-order-harmonic generation without causing undesired ionization. Moreover, the recently discovered techniques to synthesize and shape femtosecond pulses from infrared frequencies up to the extreme ultraviolet regime are rapidly extending the experimental flexibility of pulse tailoring.

Generally, we have found that the ionization can be significantly suppressed by modifying the laser pulses with optimal control theory while the fluence and the pulse length are kept fixed. For this purpose, maximizing the ground-state occupation at the end of the pulse works well as a target functional. We have shown that in the low-frequency (up to infrared) regime the ionization can be suppressed by simply avoiding high peaks in the electric-field amplitude. The resulting flattening of the pulse profile leads to a significant increase of low-frequency components. In the high-frequency (ultraviolet) regime the optimization couples the pulses with the (de)-excitations in the system. In that case the varying parameters are the pulse envelopes and/or the frequencies, while the peak intensities do not necessarily change.

Finally, we have examined whether the ground-state occupation at the end of the pulse could also be a useful target for enhancing the yield and/or the cutoff of the high-order-harmonic generation. Our results demonstrate that the optimization leads to a relatively strong overall high-order-harmonic generation yield and to the absence of clear cutoffs. However, our results in this respect are only suggestive. For future studies we propose combining the present target with other functionals, e.g., the maximization of the electric current at the end of the pulse.

## ACKNOWLEDGMENTS

This work was supported by the NordForsk Researcher Network "Time-domain quantum processes studied by ultrafast pulses," the Danish Research Council (Grant No. 10-085430), an ERC-StG (Project No. 277767, TDMET), and the Academy of Finland.

[1] F. Krausz and M. Ivanov, Rev. Mod. Phys. **81**, 163 (2009).
[2] M. Schultze, M. Fieß, N. Karpowicz, J. Gagnon, M. Korbman, M. Hofstetter, S. Neppl, A. L. Cavalieri, Y. Komninos, Th. Mercouris, C. A. Nicolaides, R. Pazourek, S. Nagele, J. Feist, J. Burgdörfer, A. M. Azzeer, R. Ernstorfer, R. Kienberger, U. Kleineberg, E. Goulielmakis, F. Krausz, and V. S. Yakovlev, Science **328**, 1658 (2010).
[3] K. Klünder, J. M. Dahlström, M. Gisselbrecht, T. Fordell, M. Swoboda, D. Guénot, P. Johnsson, J. Caillat, J. Mauritsson, A. Maquet, R. Taïeb, and A. L'Huillier, Phys. Rev. Lett. **106**, 143002 (2011).
[4] M. Uiberacker, Th. Uphues, M. Schultze, A. J. Verhoef, V. Yakovlev, M. F. Kling, J. Rauschenberger, N. M. Kabachnik, H. Schröder, M. Lezius, K. L. Kompa, H.-G. Muller, M. J. J. Vrakking, S. Hendel, U. Kleineberg, U. Heinzmann, M. Drescher, and F. Krausz, Nature (London) **446**, 627 (2007).
[5] M. F. Kling, Ch. Siedschlag, A. J. Verhoef, J. I. Khan, M. Schultze, Th. Uphues, Y. Ni, M. Uiberacker, M. Drescher, F. Krausz, and M. J. J. Vrakking, Science **312**, 246 (2006).
[6] G. G. Paulus, F. Lindner, H. Walther, A. Baltuška, E. Goulielmakis, M. Lezius, and F. Krausz, Phys. Rev. Lett. **91**, 253004 (2003).
[7] A. Wirth, M. Th. Hassan, I. Grguras, J. Gagnon, A. Moulet, T. T. Luu, S. Pabst, R. Santra, Z. A. Alahmed, A. M. Azzeer, V. S. Yakovlev, V. Pervak, F. Krausz, and E. Goulielmakis, Science **334**, 195 (2011).
[8] A. P. Peirce, M. A. Dahleh, and H. Rabitz, Phys. Rev. A **37**, 4950 (1988); R. Kosloff, S. A. Rice, P. Gaspard, S. Tersigni, and D. J. Tannor, Chem. Phys. **139**, 201 (1989).
[9] For recent reviews, see J. Werschnik and E. K. U. Gross, J. Phys. B **40**, R175 (2007); C. Brif, R. Chakrabarti, and H. Rabitz, New J. Phys. **12**, 075008 (2010).
[10] A. Castro, E. Räsänen, A. Rubio, and E. K. U. Gross, Europhys. Lett. **87**, 53001 (2009).
[11] M. J. D. Powell, *Large-Scale Nonlinear Optimization* (Springer, New York, 2004), pp. 255–297.
[12] J. Werschnik and E. K. U. Gross, J. Opt. B **7**, S300 (2005).
[13] M. Lein, J. Mod. Opt. **58**, 1188 (2011).
[14] D. G. Lappas and R. van Leeuwen, J. Phys. B **31**, L249 (1998).
[15] A. Castro and M. A. L. Marques, Lect. Notes Phys. **706**, 197 (2006).
[16] M. A. L. Marques, A. Castro, G. F. Bertsch, and A. Rubio, Comput. Phys. Commun. **151**, 60 (2003); A. Castro, H. Appel, M. Oliveira, C. A. Rozzi, X. Andrade, F. Lorenzen, M. A. L. Marques, E. K. U. Gross, and A. Rubio, Phys. Status Solidi B **243**, 2465 (2006).
[17] L. V. Keldysh, Zh. Eksp. Teor. Fiz. **47**, 1945 (1964) [Sov. Phys. JETP **20**, 1307 (1965)].
[18] J. L. Krause, K. J. Schafer, and K. C. Kulander, Phys. Rev. Lett. **68**, 3535 (1992); P. B. Corkum, *ibid.* **71**, 1994 (1993).
[19] C. Winterfeldt, C. Spielmann, and G. Gerber, Rev. Mod. Phys. **80**, 117 (2008).
[20] M. Lewenstein, P. Balcou, M. Y. Ivanov, A. L'Huillier, and P. B. Corkum, Phys. Rev. A **49**, 2117 (1994).